KfK 4348
Februar 1988

Characterization of CR 39 Nuclear Track Detector for Use as a Radon/Thoron Dosemeter

S. Kandaiya
Hauptabteilung Sicherheit

Kernforschungszentrum Karlsruhe

KERNFORSCHUNGSZENTRUM KARLSRUHE

Hauptabteilung Sicherheit

KfK 4348

CHARACTERIZATION OF CR 39 NUCLEAR TRACK DETECTOR FOR USE AS A RADON/THORON DOSEMETER

S. Kandaiya

Kernforschungszentrum Karlsruhe GmbH, Karlsruhe

Kernforschungszentrum Karlsruhe GmbH
Postfach 3640, 7500 Karlsruhe 1

ISSN 0303-4003

ABSTRACT

For the estimation of radon, thoron and their short-lived daughter products in air radon diffusion chambers with passive alpha track etch detectors have been used. The report describes the properties of CR 39 track etch detectors in particular with respect to the spectrometric detection of alpha particles in the energy range up to 8.77 MeV using chemical and a combination of chemical-electrochemical etching technique. In order to optimize the etching conditions for an α-energy discrimination in the energy range up to 8.77 MeV, the ECE track size diameter and the track density have been investigated as a function of the chemical pre-etching time using three electrical field strengths.

In a mixed α-spectrum the contributions of various α-particles with energies between 4.6 to 8.77 MeV have been determined experimentally in CR 39 and compared with the spectral measurement using a surface barrier detector and the same irradiation geometry.

Beside CR 39 detectors etched chemically and electrochemically, in addition surface barrier detectors and a Monte Carlo calculation have been used to evaluate the α-energy spectrum for thoron and its daughter products emitted by alpha decays in the air volume and the plate-out of daughters at the inner surface on the diffusion chamber.

Charakteristik von CR 39 - Kernspurätzdetektoren für die Anwendung als Radon-/Thorondosimeter

ZUSAMMENFASSUNG

Für den Nachweis von Radon, Thoron und deren kurzlebigen Tochterprodukten in Luft werden Radondiffusionskammern mit passiven Alpha-Kernspurdetektoren eingesetzt. Der Bericht beschreibt die Eigenschaften des Kernspurdetektors CR 39 insbesondere hinsichtlich eines spektrometrischen Nachweises von Alphateilchen im Energiebereich bis 8,77 MeV. Zur Optimierung der Ätzbedingungen für eine α-Energiediskriminierung wurde der Kernpurdurchmesser und die Kernspurdichte in Abhängigkeit von der chemischen Vorätzzeit bei drei verschiedenen elektrischen Feldstärken untersucht.

Für ein Gemisch von Alphaspektren wurden die Anteile verschiedener α-Teilchen mit Energien zwischen 4.66 und 8,77 MeV in CR 39 untersucht und mit einer spektroskopischen Messung unter Verwendung eines Oberflächensperrschichtdetectors in derselben Geometrie verglichen.

Für die halbkugelförmige KfK-Radondiffusionskammer wurden neben CR 39-Kernspurdetektoren mit chemischer und elektrochemischer Ätzung auch Halbleiterdetektoren und eine Monte-Carlo-Rechnung angewandt, um das α-Energiespektrum von Thoron und seinen Folgeprodukten auszuwerten, das von α-Zerfällen im Luftvolumen der Kammer und den an der Innenoberfläche abgeschiedenen Tochterprodukten herrührt.

Table of Contents

1. INTRODUCTION

In uranium mines and also in residences, it is found that inhalation of radon and its short-lived daughter products pose a health hazard. The solid state nuclear track detector (SNTD) is a passive detector, which gives an integrated dose measurement of radon/thoron and its daughter products. Bare detectors were found to have an effective sensitivity as well as a reproducibility that varied by more than a factor of 3 (Urban and Piesch, 1981) (27). It is therefore recommended that closed diffusion chambers be used for measurement of radon/thoron and its daughter nuclides.

The Karlsruhe track etch dosemeter (28) is adopted for the study. At present, the detector Makrofol is the detector in the dosemeter. However, the sensitivity of the detector is between 0.5 and 2.5 MeV.

In our study, the SSNTD CR 39 manufactured by Pershore Moulding and by American Acrylics were selected. The CR 39 in general has a much higher sensitivity from 0.5 MeV to 8.78 MeV for α-particles (Al-Najjar, 1982) (4). Before the detectors can be used in the Karlsruhe track etch dosemeter, the optimum conditions for alpha detectors have to be determined.

The project is divided into two sections, namely:

- Determination of optimum conditions for both CR 39 detectors for alpha detection.
- Measurement of thoron and its short-lived daughters using the Karlsruhe dosemeter where the Makrofol detector is replaced by the CR 39 detector.

2. DETERMINATION OF OPTIMUM ETCHING CONDITIONS FOR ALPHA PARTICLE DETECTION IN CR 39

Etching conditions are generally known to affect detector registration efficiency (Fleischer et.al., 1965 (12), Benton and Collver, 1967 (6)). To achieve optimum etching conditions for better efficiency and for higher resolution of particle detection in SSNTD, it is necessary to study the various etching parameters. The necessary parameters chosen for our work are as follows:

- Bulk etching,
- electrochemical etching,
- alpha particle spectromentry using chemical etching.

2.1 Bulk etching rate V_B

2.1.1 Method of V_B determination

The etching process in SSNTDs can be described by two velocities; (1) the bulk etching rate V_B and (2) the etching rate along the charged particle damage trail V_T. The bulk etching rate is the rate of removal thickness of the detector by an etchant. The track etching rate V_T is the removal of detector along the track path and is dependent upon the amount of energy deposited along the track.

The bulk etching rate V_B is known to depend mainly upon the detector composition and etching condition. The environmental conditions may also have an effect on the V_B value. It is therefore recommended to measure V_B for any detector material to be used.

V_B is normally and accurately determined by using the fission track diameter method. In this method the detector sample is irradiated with a collimated beam of fission fragments from a californium-252 (^{252}Cf) source directed normally to the detector surface. Then a sufficient number of fission track diameters are measured at known intervals of etching times.

The track diameter, d, is related to the etching time by the equation given by Fleischer and Price (1963) (11).

$$d = 2V_B t \sqrt{\frac{V_T - V_B}{V_T + V_B}} \qquad (1)$$

where V_T and V_B are considered as constants. In the case of fission fragments, $V_T >> V_B$, then (1) can be written as

$$d = 2V_B t$$

$$\text{or } V_B = 1/2\ d/t$$

V_B is then calculated from the slope of the d vs. t graph.

In this work, V_B was studied as a function of temperature and concentration using two etchants, i.e. sodium hydroxide (NaOH) and potassium hydroxide (KOH). The concentrations of NaOH and KOH were 5 M, 6 M and 7 M and the temperatures chosen were 30° C, 50° C and 60° C. V_B was evaluated for two detectors. i.e. CR 39 Pershore Moulding (PM) and CR 39 American Acrylics (AA).

2.1.2 V_B as a function of temperature and concentration

It has been found that the relationship between V_B and the etchant temperature T (in degree kelvin) can be expressed by an empirical equation (Frank and Benton, 1970 (13), Blandford et.al., 1970 (7), Al-Najjar et.al., 1979 (3)).

$$V_B(M) = A \exp(-E_B/kT) \qquad (2)$$

where A = constant

E_B = activation energy for the surface reaction

k = Bolzmann constant

For the two types of detector, i.e. CR 39 PM and CR 39 AA, V_B was studied for a range of temperatures and concentrations for two etchants KOH and NaOH. V_B was determined by the fission track diameter method at the different conditions.

Figures 1 and 2 show the plot of V_B against reciprocal etching temperature (1/T) for etchant KOH and NaOH, respectively. This was performed for CR 39 PM. Each V_B value was calculated from the slope of the graph of d against etching time for each concentration and temperature. Plot of d against time is shown in Figure 3 for 5 M, 6 M and 7 M KOH at 60° C.

Tab. 1 E_B as a function of concentration for the two etchants for the two types of detectors

Type of Etchant		
	CR 39 PM	CR 39 AA
KOH	E_B(eV)	E_B(eV)
5 M	0.6901 ± 0.0414	0.7017 ± 0.0421
6 M	0.6799 ± 0.0408	0.6968 ± 0.0418
7 M	0.6927 ± 0.0416	0.6930 ± 0.0416
Average Value	0.6876 ± 0.0713 = 0.69 ± 0.07	0.6972 ± 0.0725 = 0.70 ± 0.07
NaOH		
5 M	0.6986 ± 0.0419	0.7209 ± 0.0133
6 M	0.7051 ± 0.0423	0.7442 ± 0.0447
7 M	0.7126 ± 0.0428	0.7523 ± 0.0769
Average Value	0.7054 ± 0.0733 = 0.71 ± 0.07	0.7391 ± 0.0769 = 0.74 ± 0.08

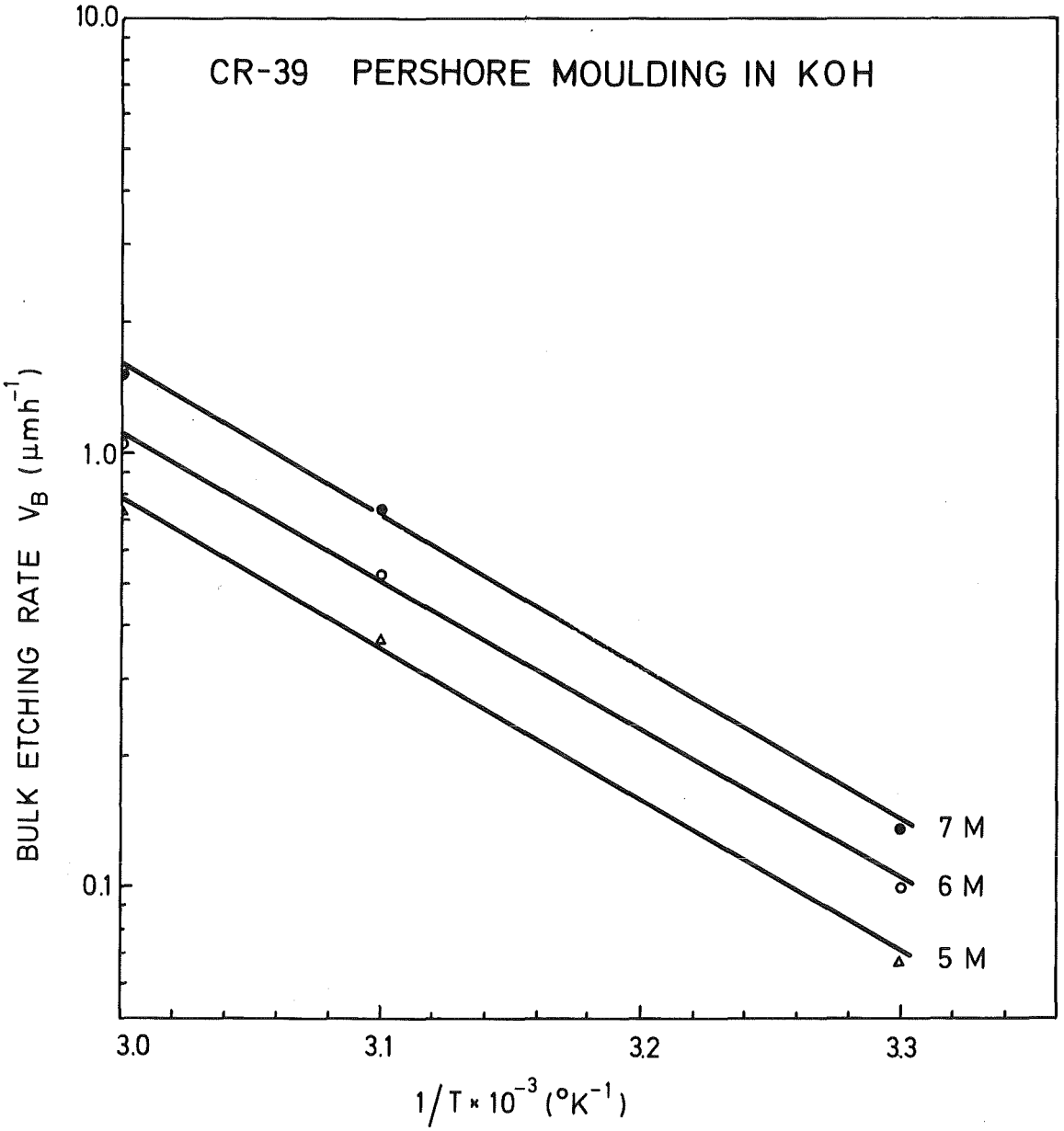

Fig. 1: Bulk etching rate of CR 39 PM against (1/T)

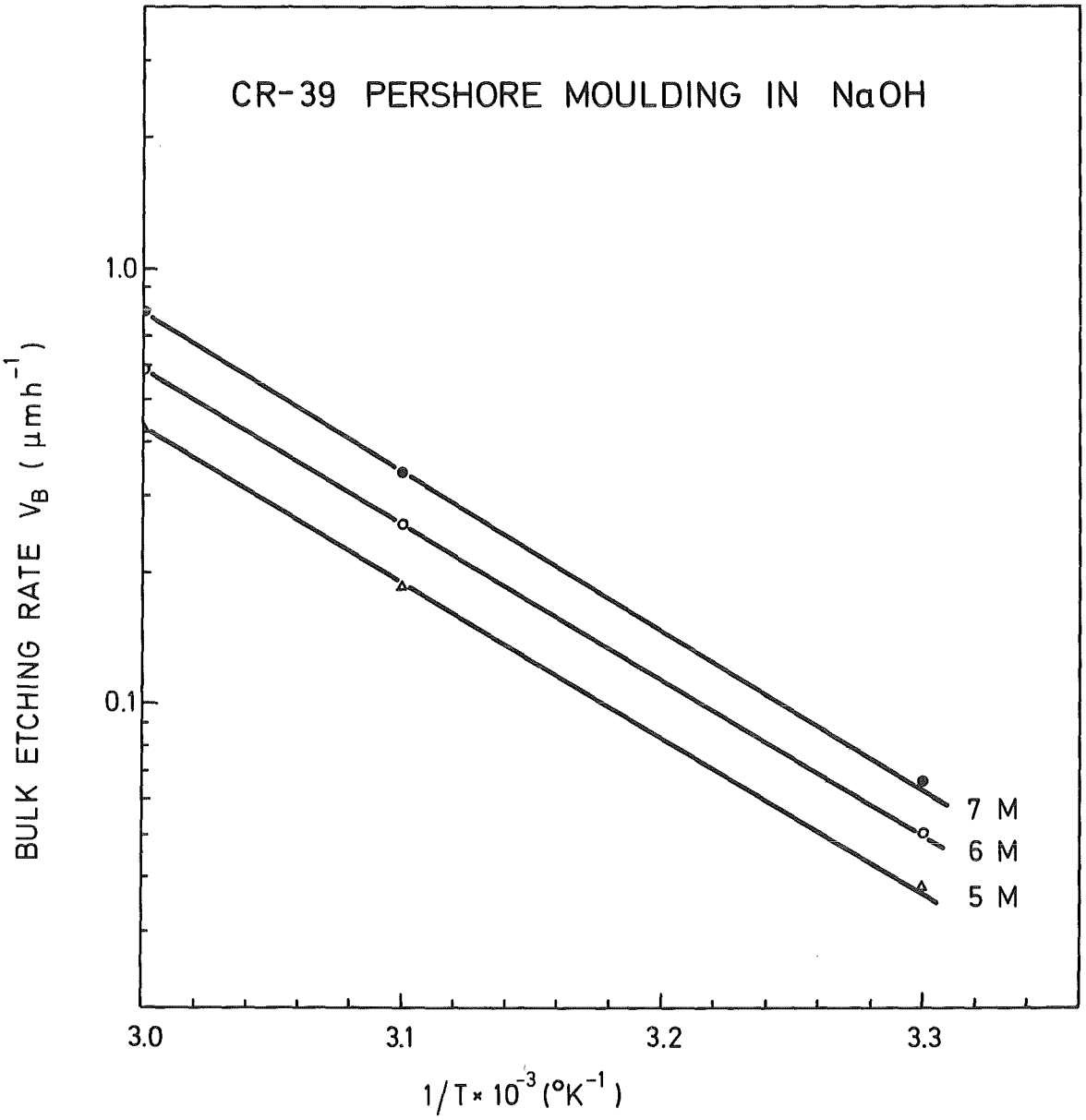

Fig. 2: Bulk etching rate of CR 39 PM against (1/T)

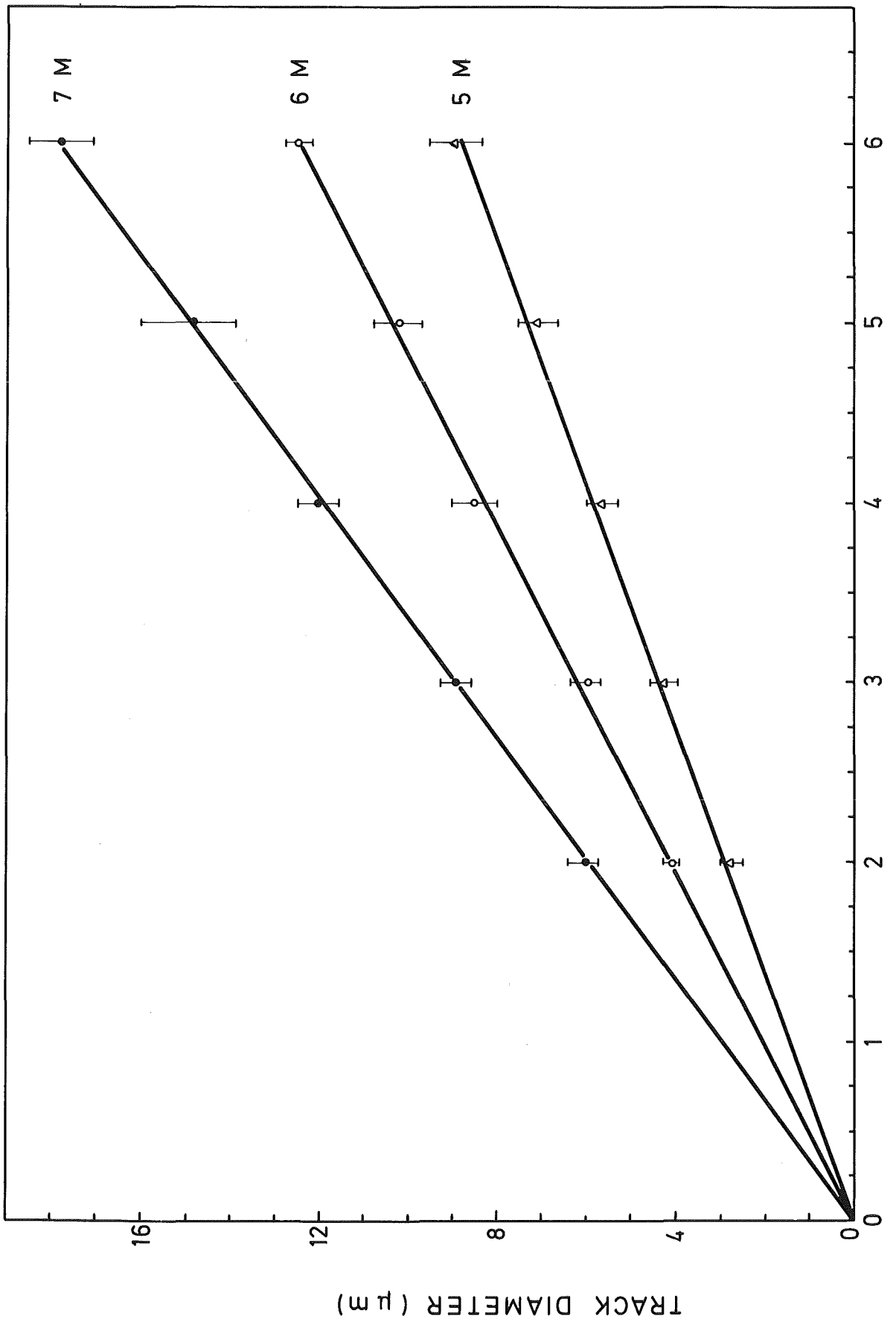

Fig. 3: Rate of fission fragment diameter growth in CR 39 PM at 60° C in 6N KOH

The activation energy E_B is calculated from the slope of graphs in Fig. 1 and Fig. 2 for CR 39 PM. A similar procedure was followed for CR 39 AA to calculate the E_B values. The values are tabulated in Tab. 1.The calculated error is from measuring statistics of the track diameter. The maximum standard deviation in track diameter gave a 6 % uncertainty.

Within the experimental error, the activation energy of each detector can be considered to be independent of the concentration of each etchant. We can also conclude that the activation energy is independent of the type of etchant used in the experiment. The E_B values obtained in the experiment are in broad agreement with other published values for CR 39 PM, for NaOH $E_B = 0.77 \pm 0.02$ eV (Green et.al., 1982) (14) ,$E_B = 0.88 \pm 0.03$ eV (Somogyi and Hunyadi, 1979) (23), $E_B = 0.78 \pm 0.03$ eV (Amin and Henshaw, 1981) (5) and for KOH $E_B = 0.76 \pm 0.03$ eV (Green et.al., 1982) (14). The slight differences in the values of E_B are due to the different conditions and doping materials added during the manufacture of CR 39. This would indicate that the activation energy is a strong function of temperature. Between the two CR 39s, there is no difference in the E_B values.

As found in a number of studies, the V_B increases with etchant concentrations (Cartwright et.al., 1978 (8), Somogyi and Hunyadi, 1979 (23), Green et.al., 1982 (14)). At all temperatures the bulk etch rate for a given molarity of KOH is greater than that of the same molarity of NaOH. This is in agreement with the data obtained in the above quoted studies. Higher bulk etching rate is obtained in KOH than in NaOH because the reactivity of these solutions increases in the order KOH > NaOH (Gruhn et.al., 1979) (16).

2.2 Alpha particle spectrometry using chemical etching

For α-particle spectrometry, the detectors have to be first calibrated with α-particles of varying energies. The calibration method is based on the fact that particles of different energies entering the surface at right angles show different track diameters for a given etching time (Somogyi and Schlenk, 1970) (20).

In the experiment the CR 39 foils (PM and AA) were irradiated with normally incident monoenergetic α-particles emitted by a thin ^{241}Am source. The α-particle energy was degraded to 1 MeV, 2 MeV, 3 MeV and 4 MeV by varying the air pressure in a vacuum chamber. A surface-barrier detector fixed in the same position as the track etch detectors, was connected to a multichannel analyser which was previously calibrated with standard α-sources.

The irradiation chamber designed for the experimet is similar to that of Al-Najjar (1982) (4). In this chamber design, 5 to 8 detectors, depending on the

size, can be irradiated at one time without re-admitting air.

Each detector was then etched in 6M KOH at 60° C for varying intervals of time. The diameters of the tracks were then measured under an optical microscope.

Track diameter growth in CR 39 PM against time for α-particle of energy 1 MeV, 2 MeV, 3 MeV, 4 MeV and 5.4 Mev are shown in Figure 4. The α-particles of the different stated energies can be distinctly separated after 7 hours of chemical etching.

A similar track diameter growth curve was performed for CR 39 AA. By 8 hours of chemical etching, tracks of different energy were separated although track diameters of 1 MeV and 2 MeV were not clearly resolvable.

The etching time curves for different α-energies cross at certain etching times. Thus α-energy can be determined from a single measurement of track diameter only when a few microns have been removed from the detector surface, i.e. before the curves start overlapping. Here, the optimum time for α-energy particle determination would be between 7 and 8 hours of etching time for both detectors.

2.3 Alpha particle spectrometry using electrochemical etching

2.3.1 Experimental procedure

For various practical applications it is necessary to enlarge the tracks formed in SSNTD in order to reduce time spent on the optical microscope. This has been achieved by electrochemical etching (Tommasino, 1970 (26); Sohrabi, 1974 (19); Somogyi, 1977 (22); Griffith et.al., 1977 (15); Al-Najjar et.al., 1978 (2)).

Electrochemical etching (ECE) occurs in two stages. First, an etch-cone is formed by ordinary chemical etching and in the second stage the initiation and propagation of the "treeing" process takes place (Durrani and Al-Najjar, 1986) (10).

In the use of CR 39 for radon/thoron activity measurements, it is necessary to register α-particles of high energy. Makrofol and Lexan polycarbonate are unable to produce ECE spots for energies higher than 4 MeV whilst CR 39 is known to respond to a wide energy range of α-particles from 1 MeV to 8.78 MeV (Al-Najjar et.al., 1979 (3); Hassib, 1979 (18); Cross et.al., 1984 (9)). In all these studies, the approach has been to perform chemical pre-etching (CPE) followed by ECE.

In this work the optimum etching conditions, i.e. CPE followed by ECE necessary for α-particle discrimination in CR 39 PM and in CR 39 AA were

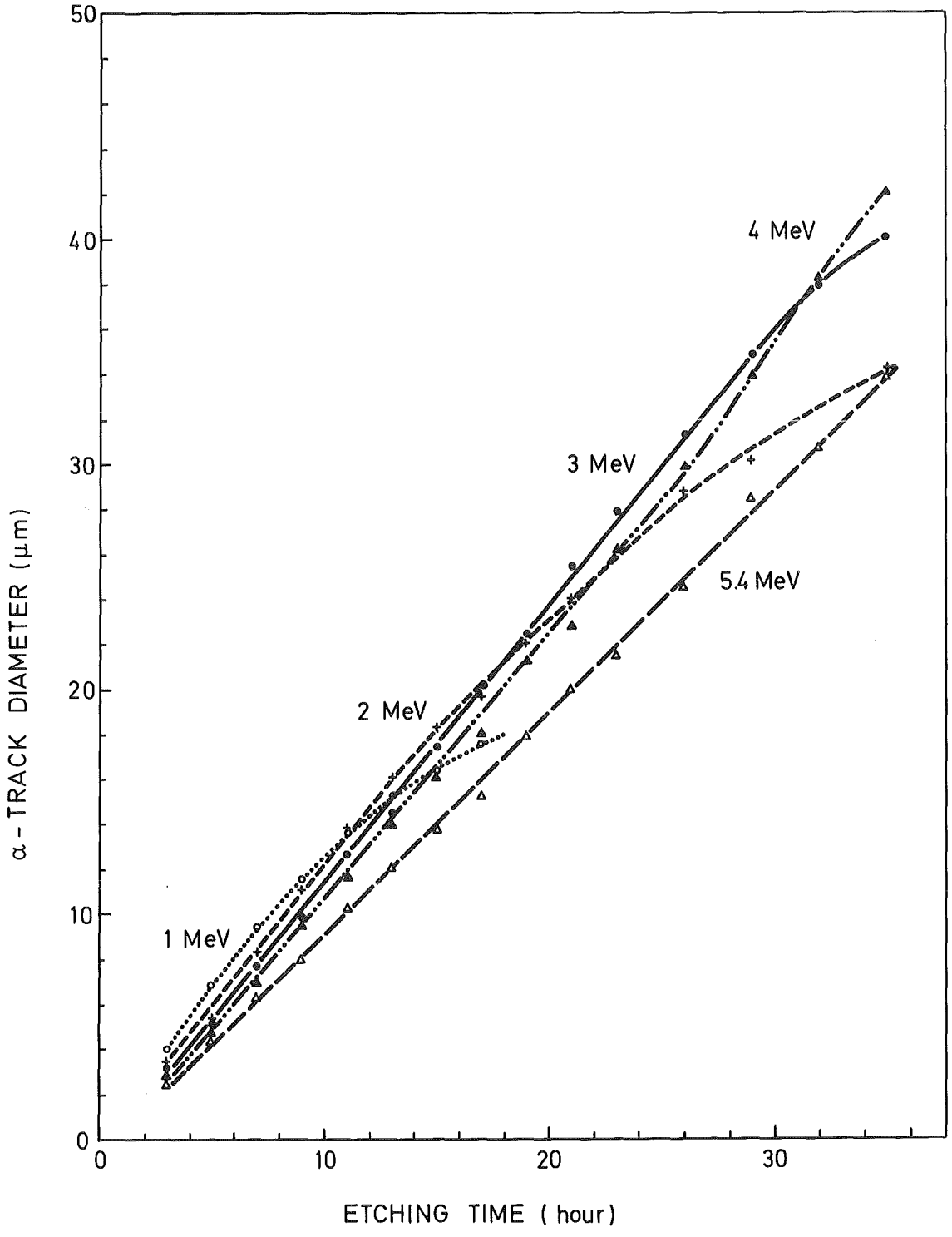

Fig. 4: Track diameter growth against etching time

studied. The two CR 39s were chosen since it has been suggested that the background produced in CR 39 AA is lower than that of CR 39 PM.

It is known that the rate of treeing breakdown is an increasing function of field strength and frequency (Somogyi, 1976 (21); Hassib et.al., 1976 (17); Al-Najjar et.al., 1978 (2)). In our laboratory, however, the maximum frequency is 5 kHz. So it was decided to fix the frequency at 2 kHz and to vary the field strength and time to produce the optimum ECE condition for α-particle discrimination.

The CR 39 sheets (both PM and AA) were cut into 2.5 cm x 2.5 cm pieces. Since CR 39 sheets were known to have variable thickness, the thickness of each sheet was measured before CPE and ECE. They were then irradiated with α-particles of different energies in the irradiation chamber.

For α-energies between 1.0 MeV and 5.4 MeV, the Am-241 source was used. To obtain α-energies between 6.0 MeV and 8.8 MeV, it was necessary to electrodeposit the daughter nuclides from a standard thoron gas source. The daughter nuclides Po-212 (8.78 MeV) and Bi-212 (6.05 MeV) were collected on a stainless steel plate by electrodeposition overnight. Alpha particle fluence to the CR 39 sheets was kept at 1500 alphas/cm^2 at all energies to avoid the effect of track density dependence on the diameter response (Sohrabi and Khajeian, 1984(25)).

The irradiated samples were first pre-etched chemically at 60° C in 6M KOH. The varying intervals of etching time selected depended on the α-energy. The samples were then etched electrochemically at 2 kHz for 2 hours and at varying field strengths of 8 kVcm^{-1}, 10 kVcm^{-1} and 15 kVcm^{-1}. The ECE was performed with 6M KOH at 60° C (± 1° C). The track diameters produced by ECE were then measured under the optical microscope. Here at least 30 isolated α-tracks are selected for track diameter measurements. The track density was also counted for each α-energy. The track density was counted over an area of 1 cm^2.

2.3.2 Efficiency and track diameter vs. pre-etching time

For each of the electric field strength selected, ECE was performed on CR 39 detectors for 2 hours. The α-particles of varying energy were discriminated as a function of chemical pre-etching time and as a function of ECE track diameter. Where discrimination was performed as a function of chemical pre-etching time, the ECE track efficiency was calculated as a function of chemical pre-etching time. The ECE track efficiency is defined as the ratio of the number of trees formed to the number of α-tracks formed by chemical pre-etching.

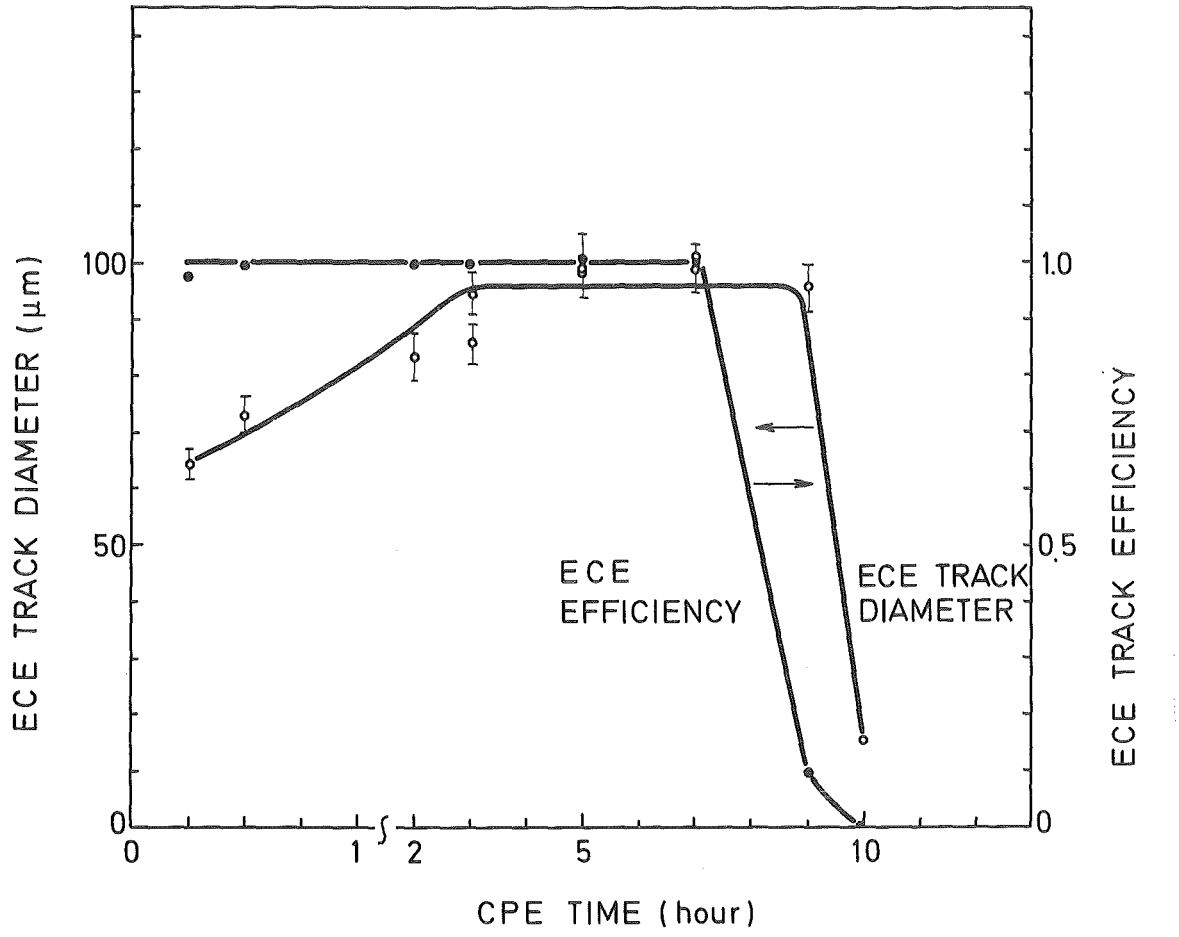

Fig. 5: ECE track diameter and ECE efficiency for 4 MeV α-particle against pre-etching time for CR 39 AA at 10 kVcm-1

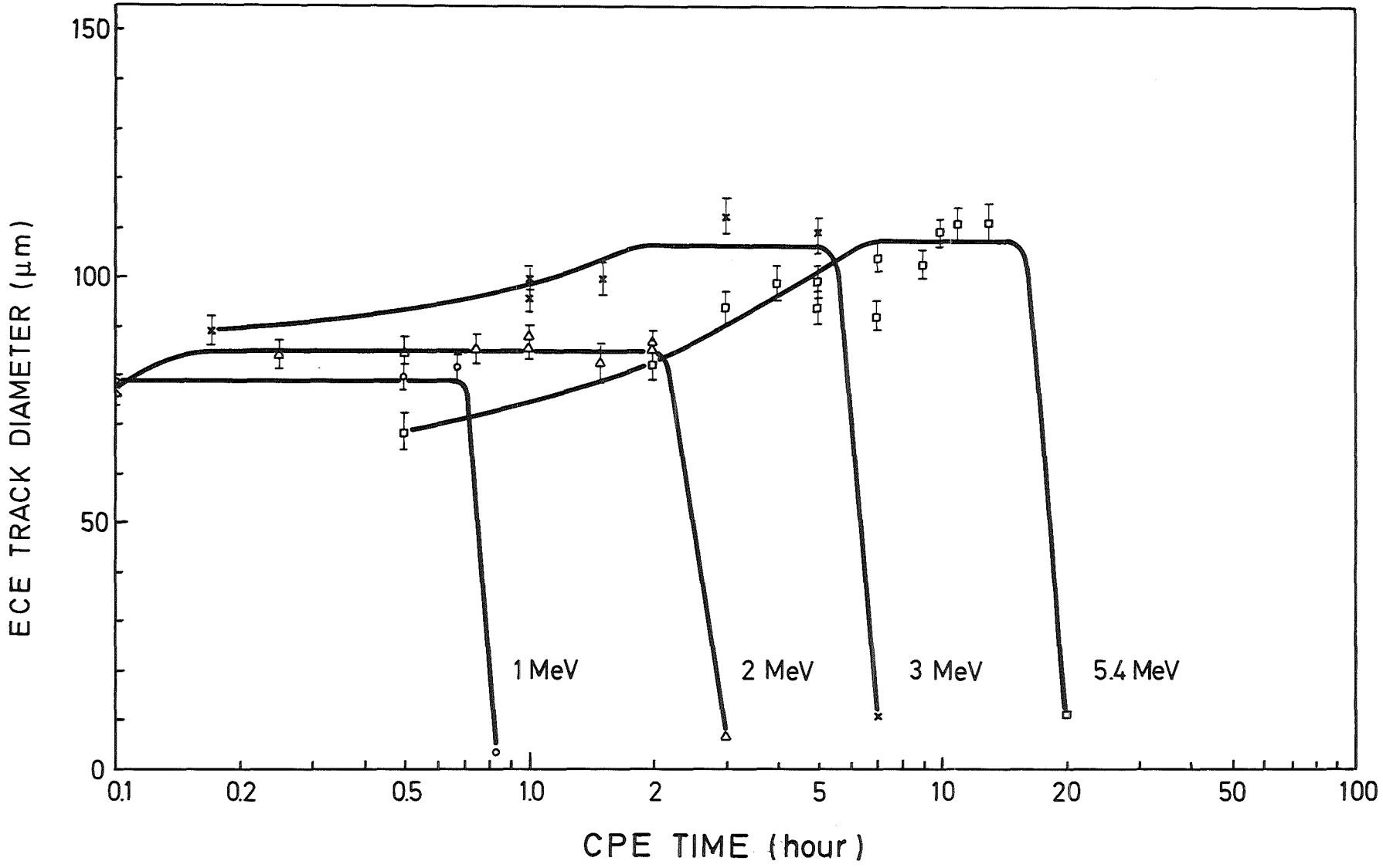

Fig. 6: ECE track diameter against pre-etching time for CR 39 AA at 10 kVcm^{-1}

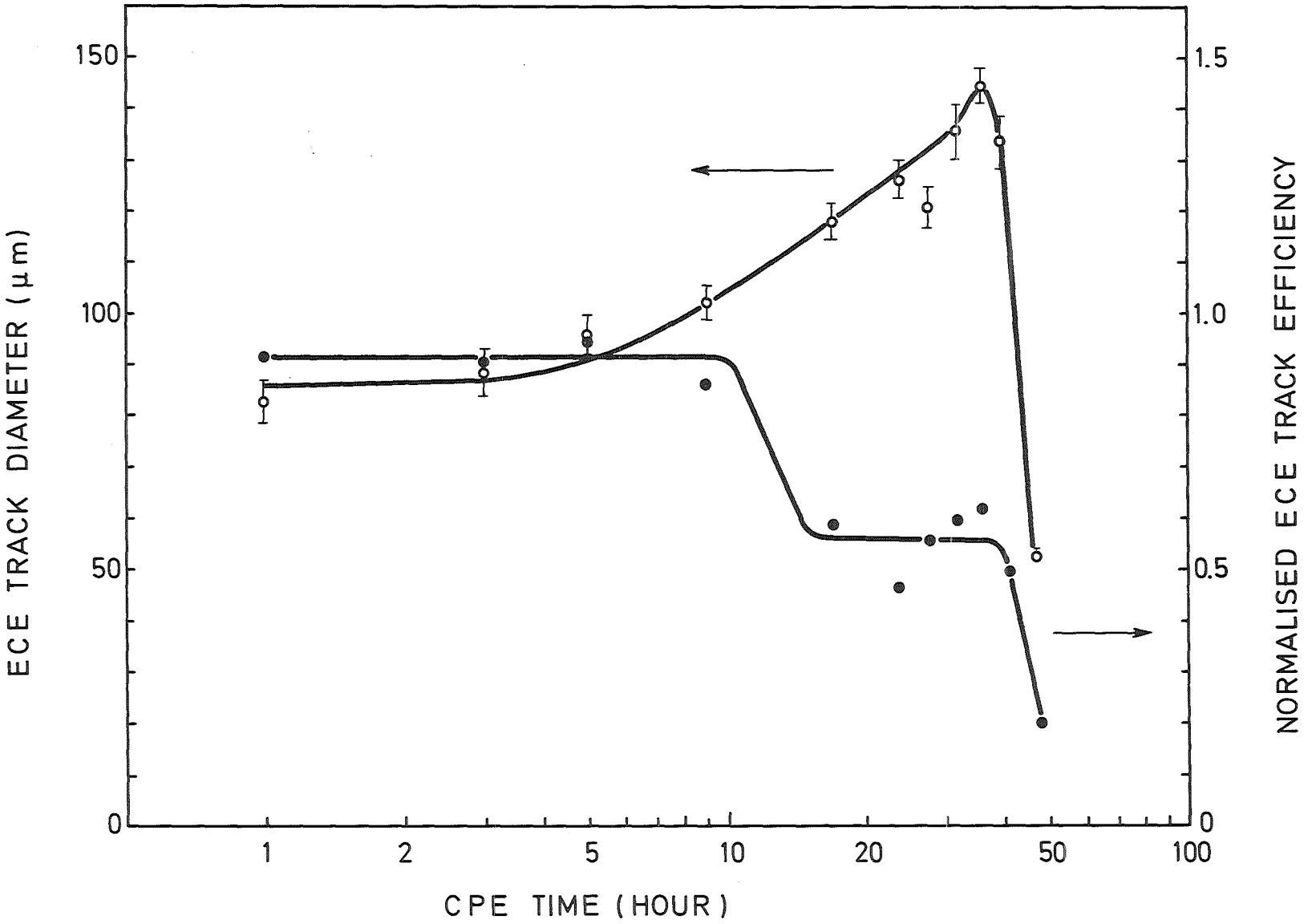

Fig. 7: ECE track diameter and ECE track efficiency for 6.1 and 8.8 MeV α-particle against CPE time for CR 39 PM at 15 kVcm^{-1}

The ECE track diameter and the ECE track efficiency for α-particle of 4 MeV in CR 39 AA is shown in Figure 5. The treeing process begins at 15 min of CPE. Here, the ECE track diameter is small. The ECE track diameter reaches its maximum size after 3 hours of CPE and this occurs when the track has been just pre-etched to its full range. The ECE track diameter then ceases to grow and begins to decline rapidly after 8 hours of CPE. At 10 hours of CPE, no trees are observed as the CPE track have reached a rounded shape. From Fig. 5, it is interesting to find that ECE track efficiency reaches its maximum value earlier than the ECE track diameter does. This implies that treeing can occur before the track has been pre-etched to its full range but this results in small ECE track diameter. The ECE track efficiency is maintained at this plateau value and then declines rapidly at the onset of rounded CPE tracks. A similar trend is observed for all α-energies, i.e. 1 MeV, 2 MeV, 3 MeV, 4 MeV, 5.4 MeV, 6.1 MeV, 7.7 MeV and 8.8 MeV in CR 39 AA and in CR 39 PM. This trend has also been observed by Durrani and Al-Najjar (1986) (10) and Abdel Naby et.al., (1986) (1) in CR 39 PM.

The ECE track diameter as a function of CPE time is shown in Fig. 6 for 1,2,3 and 5.4 MeV in CR 39 AA at 10 $kVcm^{-1}$. Fig. 7 shows both ECE track diameter and normalised ECE track density as a function of CPE time for 6.1 MeV and 8.8 MeV from thoron daughters in CR 39 PM at 15 $kVcm^{-1}$.

2.3.3 Alpha particle energy discrimination

The normalised ECE track density against CPE time curve was used for α-energy discrimination. For each α-energy, the turning point at the end of the plateau rather than the mid-point of the plateau was selected as the optimum CPE time. This gives a sharper distinction between each α-energy when the ECE method is used. The values of CPE time against energy for CR 39 PM and CR 39 AA is shown in Fig. 8 for electric field strengths of 10 $kVcm^{-1}$ and 15 $kVcm^{-1}$. Between 1 MeV and 5 MeV, there is no significant difference in CPE time with respect to the electric field strength used. From 6 MeV to 8.8 MeV, the CPE time for 15 $kVcm^{-1}$ was higher than that for 10 $kVcm^{-1}$. For 8 $kVcm^{-1}$, the CPE time was much lower than that for 10 $kVcm^{-1}$ at energies between 6 MeV and 8.8 MeV.

The slopes of the curves indicate a sharper discrimination is obtained for α-energies greater than 6 MeV at 15 $kVcm^{-1}$.

There is no significant difference in CPE times for all the α-energies when CR 39 AA and CR 39 PM were used at each of the electric field strengths. The error bars in the graph indicate the deviation in time from two experiments.

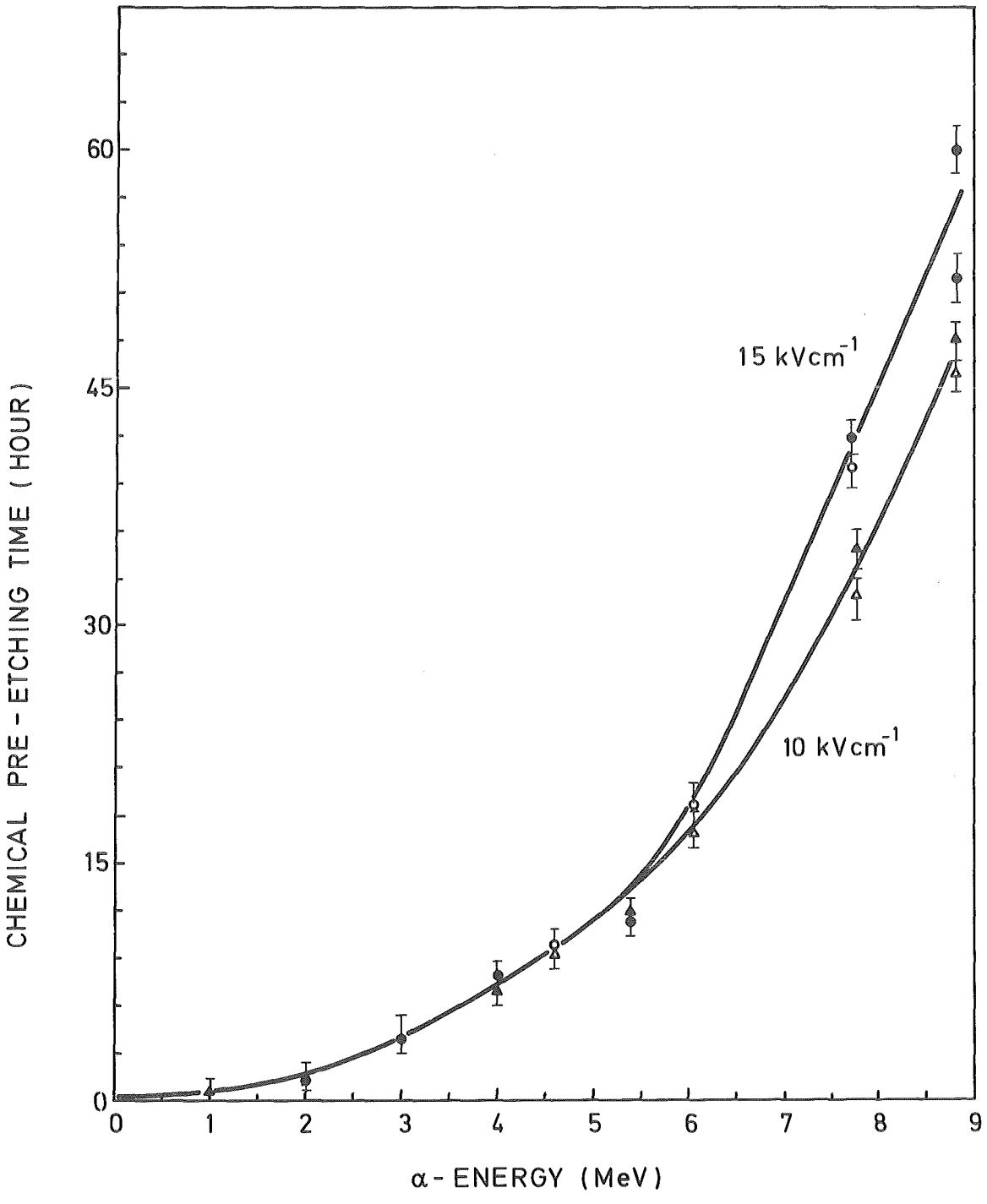

Fig. 8: CPE time against known α-energy at 10 kVcm^{-1} and 15 kVcm^{-1} for CR 39 PM (0,Δ) and CR 39 AA (●,▲)

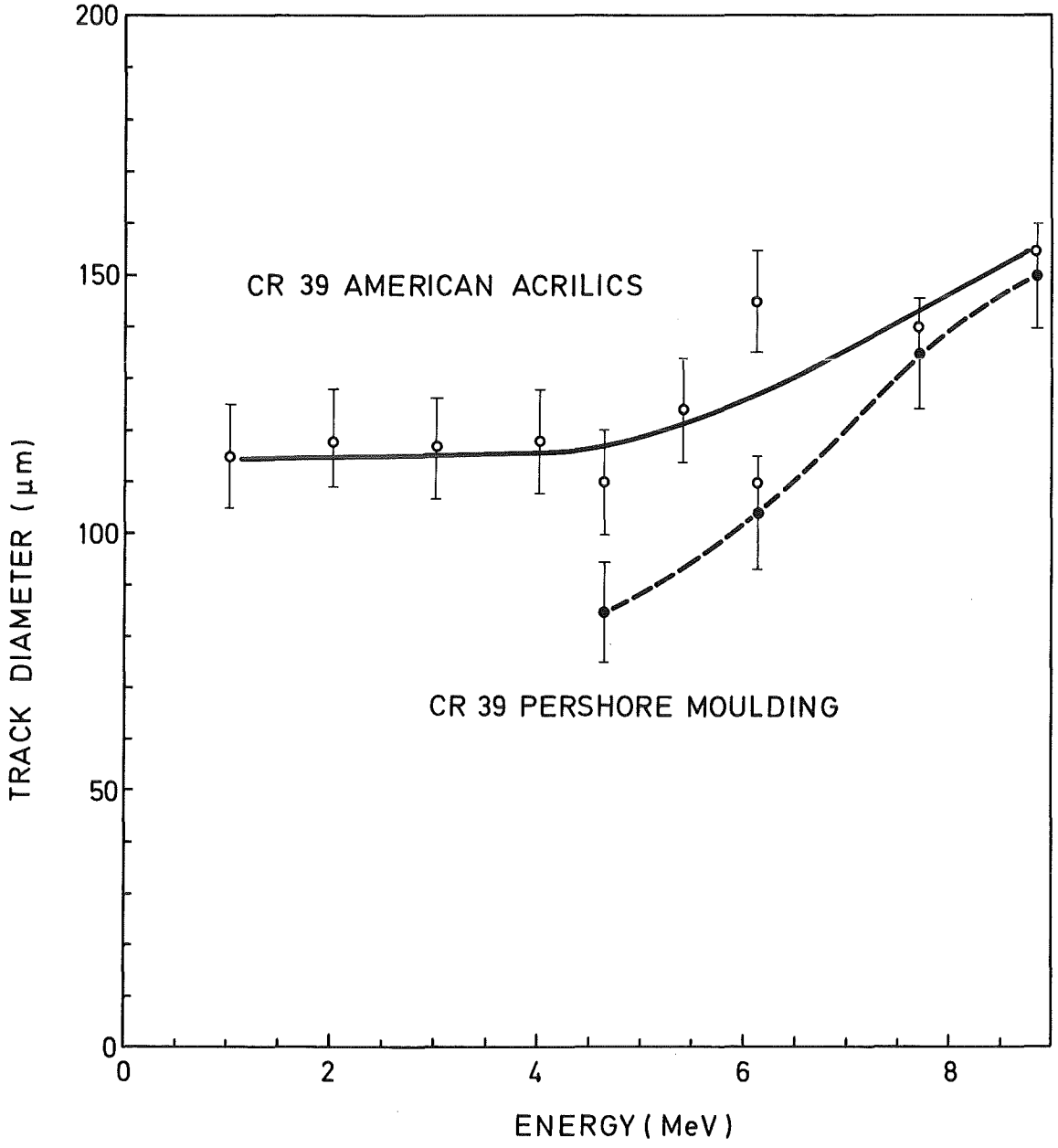

Fig. 9: ECE track diameter against α-energy at 10 kVcm-1 for CR 39 PM (●) and CR 39 AA (o)

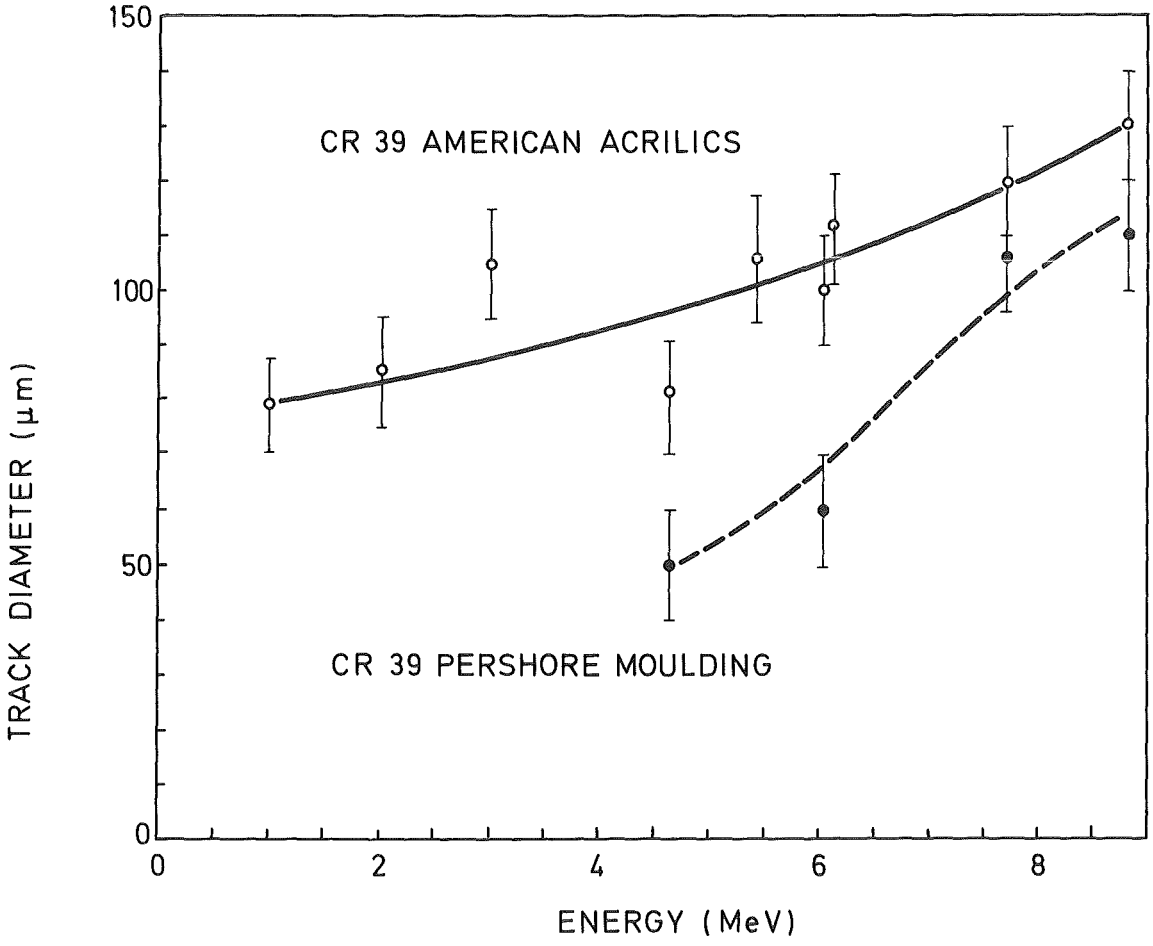

Fig. 10: ECE track diameter against α-energy at 15 kVcm^{-1} for CR 39 PM (●) and CR 39 AA (o)

The daughter nuclides of thoron and radon gas have energies between 4.6 MeV and 8.8 MeV. Hence discrimination of alpha particle energy using CPE time would be optimum at the field strength of 15 $kVcm^{-1}$.

The ECE track diameters against α-energy are plotted in Fig. 9 and Fig. 10 for electric field strengths of 10 $kVcm^{-1}$ and 15 $kVcm^{-1}$, respectively for both CR 39 PM and CR 39 AA. The error bars represent the deviations in ECE track diameter from two experiments.

The plots show that at an electric field strength of 15 $kVcm^{-1}$, separation of α-energy using ECE track diameter is possible from 1 MeV to 8.8 MeV whilst 10 $kVcm^{-1}$ separation of α-energies is only attainable after 4.5 MeV. The CR 39 PM displays a much sharper discrimination at each of the electric field strengths used. At an electric field strength of 15 $kVcm^{-1}$, the ECE track diameter was from 85 μm to 150 μm compared to ECE track diameter from 50 μm to 100 μm at 10 $kVcm^{-1}$ for a similar range of α-energy i.e. from 4.6 MeV to 8.8 MeV. A slightly better ECE track diameter range is obtained at 15 kVcm-1 in CR 39 PM. The only drawback is in the scatter of ECE track diameter which might not allow a sharp discrimination of each of the α-energy.

The ECE track diameter was measured from a minimum of 30 ECE tracks and the average ECE track diameter was calculated. A better resolution of ECE track diameter would have been obtained using an automatic scanning system. Here a track diameter spectrum of a larger number of ECE tracks would be possible.

2.3.4 Background tracks in ECE

Due to the low level counting in ECE, the number of background ECE tracks must be kept to a minimum. The background tracks at each of the electric fields were obtained from

(1) unirradiated samples which were not chemically pre-etched but kept in similar conditions as irradiated samples.

(2) irradiated samples where the CPE tracks had failed to produced ECE tracks.

The results are tabulated in Table 2. The values shown are selected randomly from five different experiments.

Tab. 2 Background ECE tracks for the selected field strengths

Electric field strength					
8 $kVcm^{-1}$		10 $kVcm^{-1}$		15 $kVcm^{-1}$	
CR 39 AA	CR 39 PM	CR 39 AA	CR 39 PM	CR 39 AA	CR 39 PM
10 ± 4	-	20 ± 7	10 ± 3	30 ± 10	15 ± 5
15 ± 7	-	24 ± 10	12 ± 4	20 ± 11	10 ± 5
8 ± 3	-	12 ± 8	17 ± 7	22 ± 8	16 ± 4
12 ± 14	-	17 ± 10	14 ± 4	15 ± 10	20 ± 8
10 ± 6	-	25 ± 8	11 ± 5	28 ± 10	14 ± 6

The track density is the number of tracks per cm^2. The standard deviation shown is obtained from four samples in each experiment.

The background track density increases with increasing electric field strength. At the selected electric field of 10 $kVcm^{-1}$ and 15 $kVcm^{-1}$, the CR 39 PM showed a slightly lower background ECE track density compared to CR 39 AA.

Based on background ECE track density and α-energy discrimination the CR 39 PM rather than CR 39 AA was selected for the latter experiments.

The field strength of 15 $kVcm^{-1}$ was chosen inspite of its slightly higher background ECE track density as it gave a better discrimination of α-energy between 4.6 and 8.8 MeV.

2.4 Energy discrimination in mixed alpha energy fields

In all the earlier experiments each CR 39 sheet was irradiated normally with a monoenergetic α-particle and then etched electrochemically. In this experiment each CR 39 PM piece was irradiated with normally incident α-particles which had either two or four different energies. The CR 39 PM was chemically pre-etched at 60° C in 6 M KOH at varying intervals of time and then etched electrochemically at 15 $kVcm^{-1}$ for 2 hours with 6 M KOH at 60° C.

The ECE track density and ECE track diameter measurements were performed as described earlier.

Fig. 11 shows the normalised ECE track density and the ECE track diameter for varying CPE time for 4.6 MeV and 7.7 MeV α-energy. Two distinct plateaus are observed for both ECE track diameter and normalised track density curves. From the ECE track diameter values, the α-energies are 4.5 MeV and 7.7 MeV. Similar α-energy values were deduced from the track density curve. However, the contribution of each α-energy can be deduced only from the track density

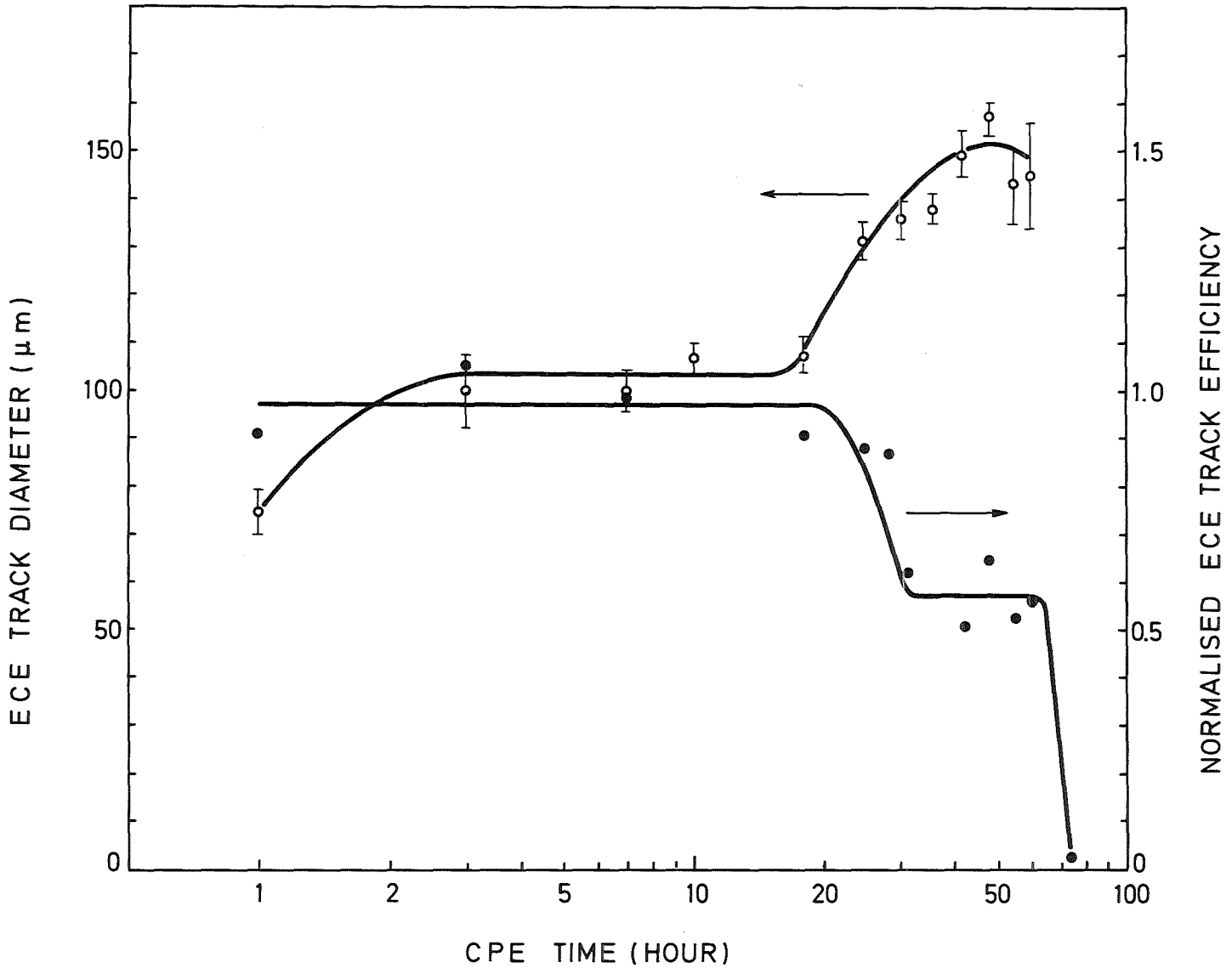

Fig. 11: ECE track diameter and ECE track efficiency for 4.6 MeV and 7.7 MeV α-particle against CPE time

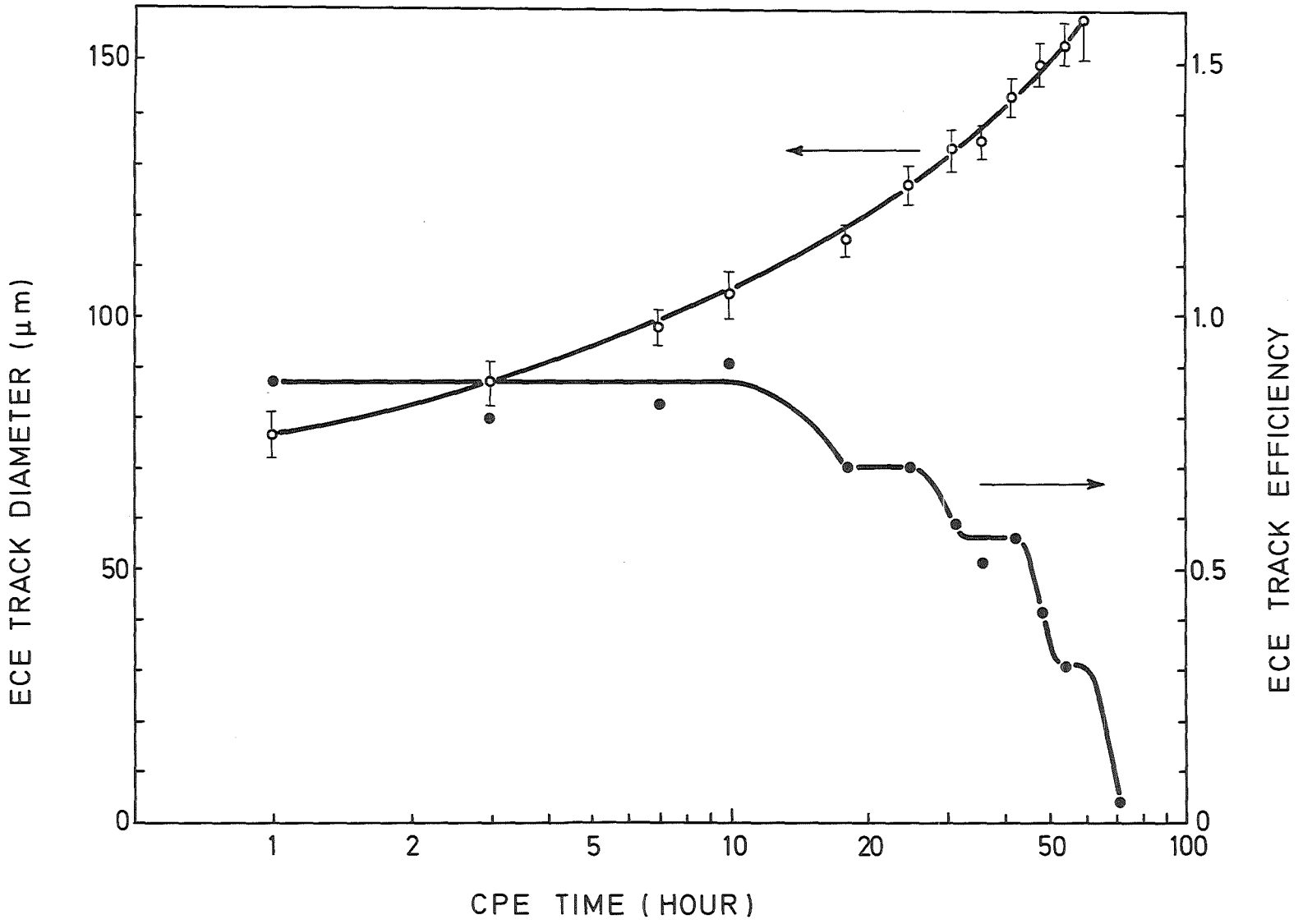

Fig. 12: ECE track diameter and ECE track efficiency for α-particle of 4.6 MeV, 6.1 MeV, 7.7 MeV and 8.8 MeV against CPE time

curve. 7.7 MeV α-energy contributes 60 % whilst 4.6 MeV α-energy contributes 40 %. The values are in agreement with those obtained using the surface barrier detector.

With four α-energies i.e. 4.6 MeV, 6.1 MeV, 7.7 MeV and 8.8 MeV, the ECE track diameter and track density for varying CPE time is shown in Fig. 12. The ECE track diameter gave a continuous curve from CPE 1 hr to CPE 60 hr. This indicates a energy range between 4.5 MeV to 8.8 MeV. In the ECE track density curve, there is an initial plateau which drops off at 10 hours. This turning point corresponds at an α-energy of 4.6 MeV. The next turning points occur at 24 hours, 41 hours and 60 hours which correspons to α-energies of 6.4 MeV, 7.7 MeV and 8.8 MeV. At these turning points, the rounded CPE tracks which have not been electrochemically etched can be observed clearly. At energies above 6.0 MeV, the energies can be read to an accuracy of 0.5 MeV from the CPE time. A 0.5 MeV energy difference corresponds to a minimum of 6 hour difference in CPE time. The deviation in determination of CPE time lies between 2-3 hours which gives rise to ± 0.25 MeV.

The contribution of each of α-energies is tabulated below with the corresponding values obtained from the surface-barrier detector.

Tab. 3 Comparison of % contribution of each α-energy between ECE and surface-barrier method

α-Energy (MeV)[1)]		Relative Contribution in %	
ECE	Surface-Barrier Detector	ECE	Surface-Barrier Detector
4.60	4.60	18	20
6.40	6.10	18	20
7.70	7.70	28	30
8.80	8.80	36	30

1) uncertainty of α-energy estimation for ECE detector ± 0.25 MeV and surface barrier detector ± 0.05

Within the error limits, the values obtained from ECE do agree with those values from the surface barrier detector.

If CR 39 PM had been irradiated with α-energies where the separation between each energy is less than 0.5 MeV, then it is possible to obtain a continuous curve without any distinct plateaus. Hence it would only be

possible to define the range of α-energy without knowing the contribution from each energy.

3. ENERGY DISCRIMINATION OF THORON DAUGHTERS IN THE KFK RADON DOSEMETER

3.1 Experimental procedure

The KfK dosemeter can be used to measure radon, thoron and its decay products. This dosemeter consists of a hemispherical housing which is 3 cm in diameter and 1.5 cm in height, a cover and a detector holder ring made from conductive plastics (Urban, 1986 (28)). The cross-section of the dosemeter is shown in Fig. 13. The CR 39 PM detector is placed in the holder ring which has a diameter of 1 cm. The dosemeter is used as an open dosemeter to measure thoron and its decay products.

A passive dosemeter placed inside the dosemeter makes use of tracksize distribution to separate and identify the different α-energy groups. In the experiments performed below, CR 39 PM is used as passive detector.

The α-energy spectrum was evaluated for daughter nuclides from a thoron source plated out on the surface of the KfK dosemeter. The energy spectrum for thoron gas and its daughter nuclides formed in the air volume and on the surface of the dosemeter was also evaluated. The energy spectrum was deduced by different methods by using

- a surface barrier detector,
- a Monte Carlo calculation,
- chemical pre-etching (CPE) combined with electrochemical etching (ECE),
- chemical etching.

3.2 Estimation of the α-energy spectrum of thoron daughter nuclides plated out on the inner surface of the KfK radon dosemeter

The walls of the hemispherical housing was electroplated with the daughter nuclides from a standard thoron gas source using a high electric field. The daughter nuclides Po-212 (8.78 MeV) and Bi-212 (6.05 MeV) were collected overnight and the contribution of Po-212 was 64 % whilst Bi-212 contributed 36 %. The cover was then put on the dosemeter. The CR 39 PM was placed on the holder ring and irradiated with the α-particles so that a track density of 1500 tracks/cm^2 are produced for ECE. In the case of only chemical etching, the track density was increased to about 10000 tracks/cm^2.

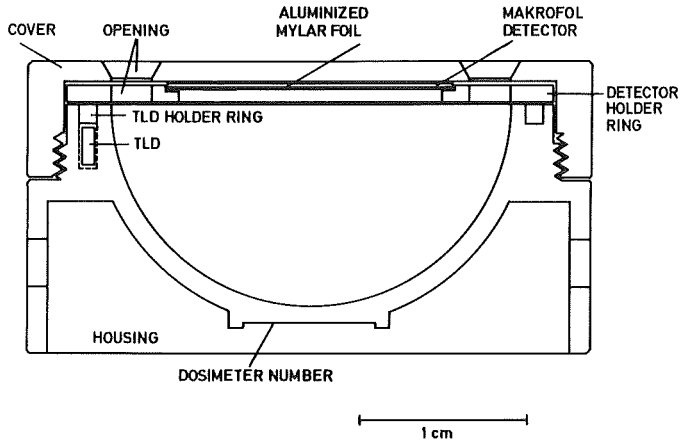

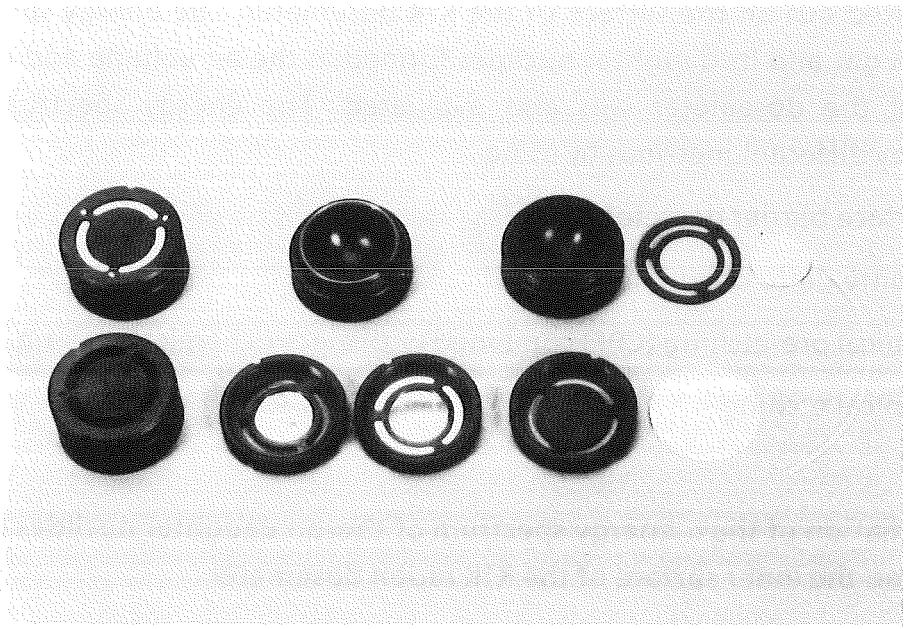

Fig. 13: The KfK radon dosemeter

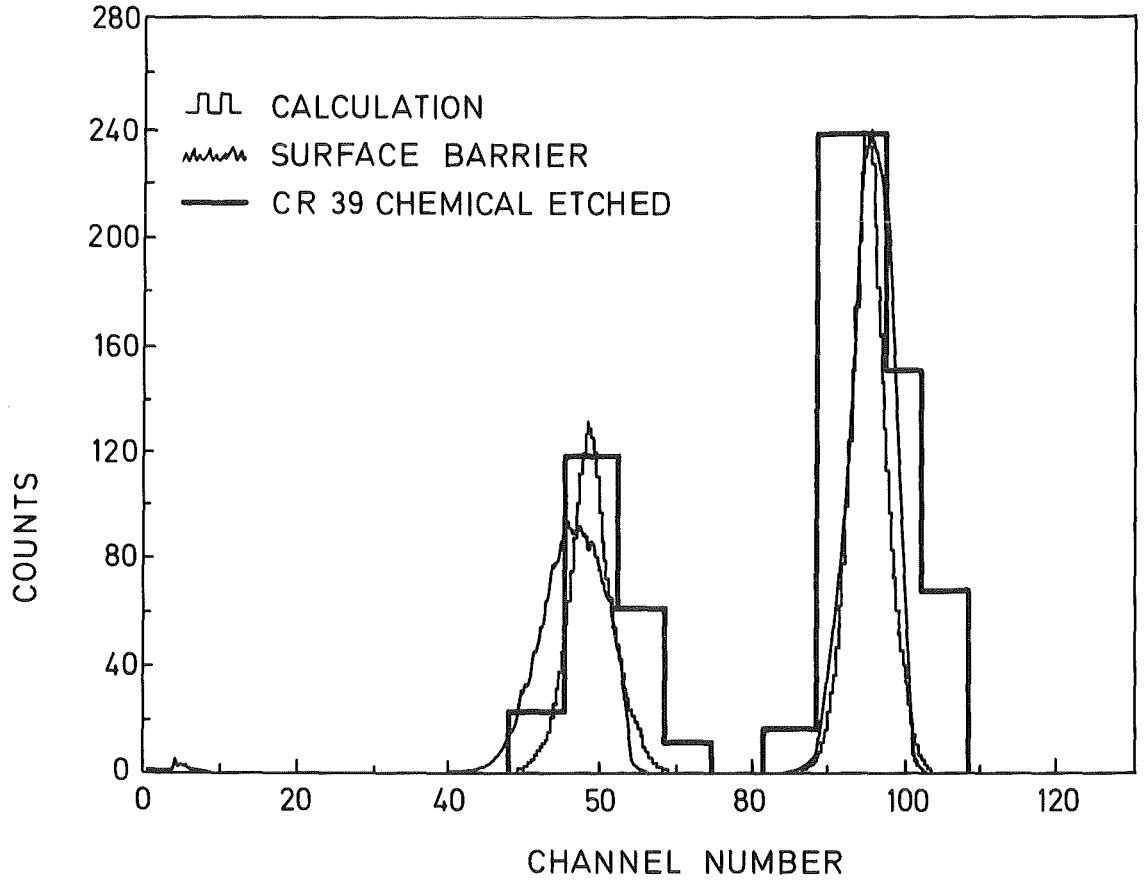

Fig. 14: Calculated and measured α-spectra of thoron daughter nuclides plated onto the wall of the KfK dosemeter

A α-spectra from Monte Carlo calculation
B α-spectra from the surface-barrier detector
C α-spectra using chemical etching

3.2.1 Energy measurement using the surface barrier detector

The surface barrier detector was placed in the position of the holder ring which has a diameter of 1 cm. The pulse height spectrum collected for 1 Ks is shown in Fig. 14. The spectrum consists of two Gaussian peaks. The peak energies occur at 4.6 MeV and at 7.7 MeV. The concentration of the two α-energies are in the ratio of 2:3.

3.2.2 Energy measurement using ECE

The irradiated samples of CR 39 PM were pre-etched chemically for varying times and then etched electrochemically at 15 kVcm^{-1} for 2 h at 60° C in 6 M KOH. The ECE track density was counted and plotted against CPE time (Fig. 15). Two distinct plateaus are observed, one is between 1 h to 10 h and the other is between 18 h and 38 h. From the turning points in the plateau, the α-energies were determined. The α-particles had energies of 4.5 MeV and 7.5 MeV. The deviation being ± 0.25 MeV for each energy. The α-particle contributions of 4.5 MeV and 7.5 MeV are 30 % and 70 % respectively.

3.2.3 Energy measurement using chemical etching

The α-particles from the daughter nuclides arrived at the detector CR 39 PM at varying angles of incidence. The chemically etched track diameter would now possess both minor and major axes since the shape of the track is an ellipse. Only the normally incident α-particles would be circular in shape. It was then necessary to measure both the minor and major axes to determine the energy of the α-particle.

To evaluate the α-energy, the following equations given by Somogyi (1980) (24) were used

$$Minor\,Axis\ d_1 = 2h\ \frac{V\sin\theta - 1}{V\sin\theta + 1} \qquad 0 < h \le h_1 = R_o(\sin\theta + \frac{1}{V})$$

$$Minor\,Axis\ D_1 = 2h\ \frac{V^2 - 1}{V\sin\theta + 1} \qquad 0 \le h \le h_1 = R_o\ \frac{(V^2-1)\sin\theta + A}{V\sin\theta + A}$$

where V = V_T/V_B = etch-rate ratio

θ = angle of incidence of particle to the detector surface

h = $V_B t$

t = etching time

$A = \cos\theta \cdot \sqrt{V^2-1}$

The equations are valid for thick isotropic solids at constant etch-rate ratio. Since the major and minor axes were measured at certain etching times, the etch-rate ratio can be assumed constant.

The values d_1 and D_1 were generated using θ-values from 0 to $\pi/2$. At $\theta = \pi/2$, $d_1 = D_1$ for a given energy. At known α-energies, d_1 and D_1 were measured under the microscope at $\theta = \pi/2$. Values of d_1 and D_1 were then generated for the other θ-values. The θ-values were taken at an interval of 10°. The computer generated curves are shown in Fig. 16 for energies between 6.1 MeV and 8.8 MeV at a chemical etching time of 32 hours. The etch rate ratio was measured for each experiment.

The irradiated CR 39 PM samples were chemically etched at 60° C in 6 M KOH for 15 h and for 32 h. The major and minor axes of 200 tracks were measured at each time. At 15 h, energy resolution from 4 MeV to 6.5 MeV was possible whilst at 32 h, better resolution was obtained for the higher energies, i.e. from 6.0 MeV to 8.8 MeV. The tracks obtained were normalised and are shown as a histogram (Fig. 14).

3.2.4 Energy spectrum from Monte Carlo calculation

Monte Carlo simulation was used to estimate the response of the track etch detector for α-particles plated onto the walls of the hemispherical chamber. The calculation is a modified program of that given by I.R. Williams (1966) (29). In the calculation it is assumed that secular equilibrium exists between the daughter nuclides and the parent nuclide. Hence the % concentration of Bi-212 is 36 % and for Po-212 is 64 %. Gaussian correction was done for the counts obtained at each energy. The program written in BASIC is given in the Appendix.

The spectrum obtained is shown in Fig. 14. Two distinct peaks at 4.6 MeV and 7.7 MeV were obtained.

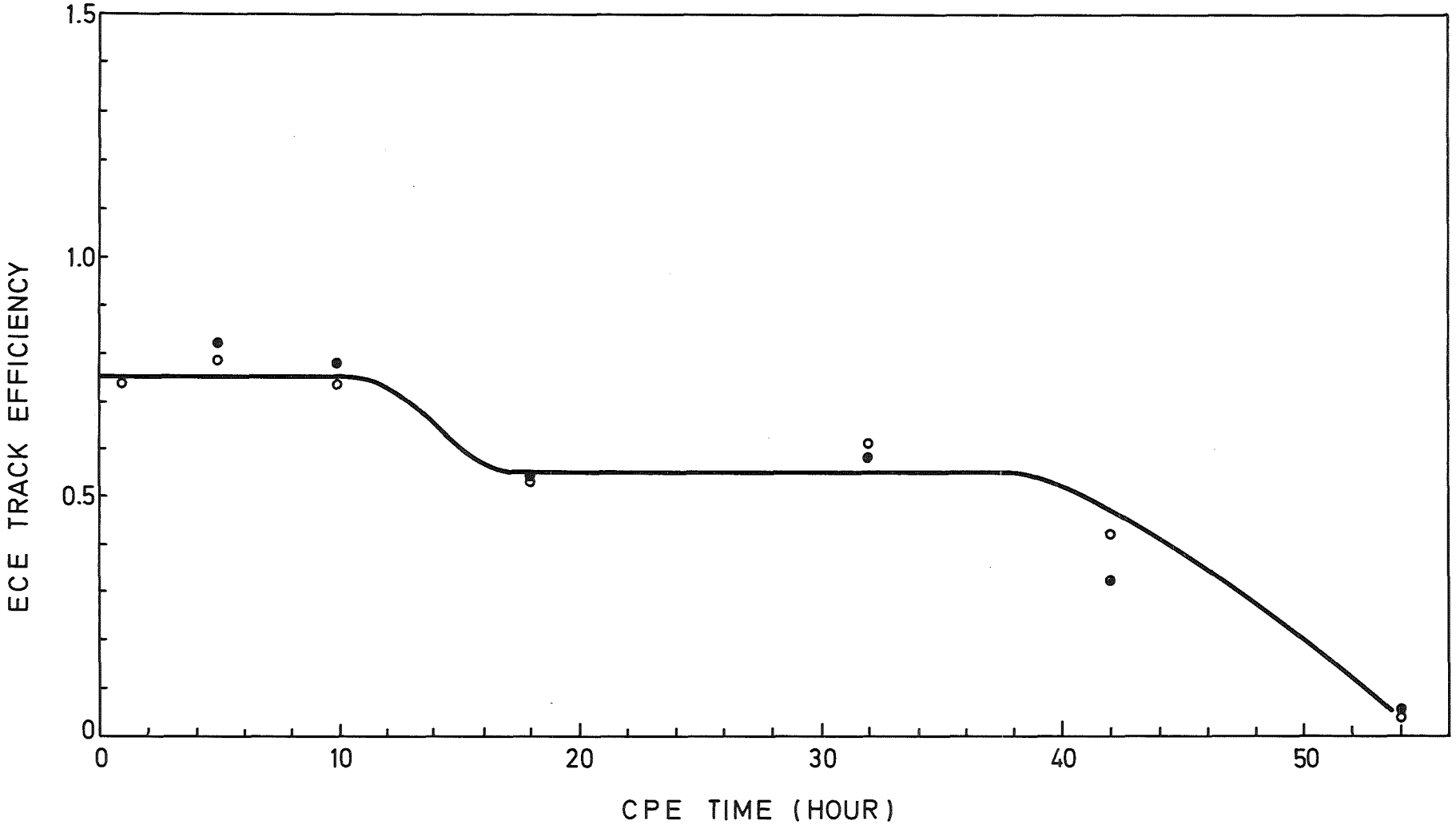

Fig. 15: ECE track efficiency against CPE time in CR 39 PM for thoron daughter nuclides plated onto the wall of the KfK dosemeter

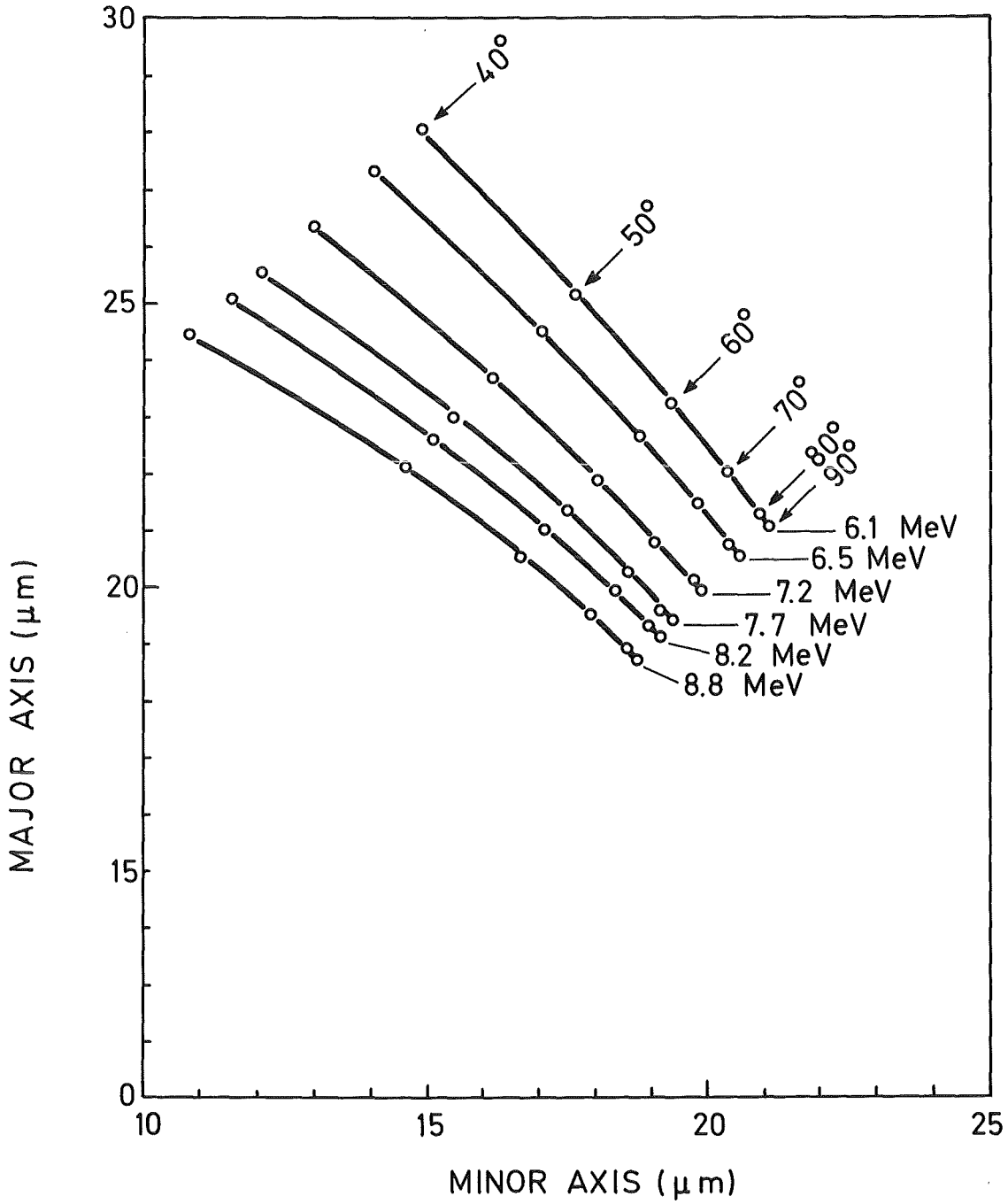

Fig. 16: Plot of major against minor axes for varying α-energies and angles θ at chemical etching time of 32 hours for CR 39 PM. Axes value for θ = 90° were obtained from experiment whilst values for other angles were obtained from calculation

3.2.5 Discussion

The energy spectrum obtained from the surface barrier detector, Monte Carlo calculation and from chemical etching only are in close agreement. The energy peaks occurred at 4.5 MeV and at 7.7 MeV. The energies of the daughter nuclides Bi-212 and Po-212 at 6.05 MeV and at 8.78 MeV, respectively, have been attenuated by air and finally arrived at the holder ring with energies of 4.6 MeV and 7.7 MeV. With ECE technique, a gross distribution is obtained. The relative concentrations in % of the α-particles at 4.5 MeV and 7.7 MeV evaluated from the surface barrier detector, from chemical etching and from ECE are in agreement.

3.3 Estimation of the α-energy spectrum of thoron gas and its daughter nuclides using the KfK dosemeter

The CR 39 PM is covered with a thin aluminised detector foil and placed in the holder ring of the KfK dosemeter without applying the diffusion filter (open chamber). The dosemeter is hung in a spherical chamber where thoron gas from a standard source is allowed to flow through. The dosemeter is placed in this chamber for about 1 hour.

The α-spectrum was evaluated using chemical etching only and compared with that obtained from Monte Carlo calculation.

Since thoron gas is emitted from a standard source it is assumed that thoron and its daughter nuclides are in secular equilibrium. In equilibrium, the energies of the daughter nuclides and % concentrations are as follows:
Rn-220 (6.29 MeV/100 %), Po-216 (6.78 MeV/100 %), Bi-212 (6.05 MeV/36 %) and Po-212 (8.78 MeV/64 %). The Monte Carlo calculation was based on these concentrations.

The calculated spectrum evaluated for chemical etching using Somogyi's equations is shown in Fig. 17. The spectrum from the Monte Carlo calculation shows two energy peaks. The first Gaussian curve spreads from 4.5 MeV to 7.0 MeV and the maxima in the curve occurs at 6 MeV and at 6.6 MeV. These correspond to radionuclides Rn-220, Po-216 and Bi-212 with energies 6.29 MeV, 6.78 MeV and 6.05 MeV, respectively. The difference in the energy is due to attenuation in air. The second Gaussian curve spreads from 7.5 MeV to 9.0 MeV, the maximum occuring at 8.6 MeV. This corresponds to Po-212 whose α-energy is 8.8 MeV. Again, there is a loss in energy due to attenuation in air.

From chemical etching, the measured energy spread is from 4.0 MeV to 8.8 MeV, the maximum occuring between 6.25 MeV and 6.8 MeV. However there

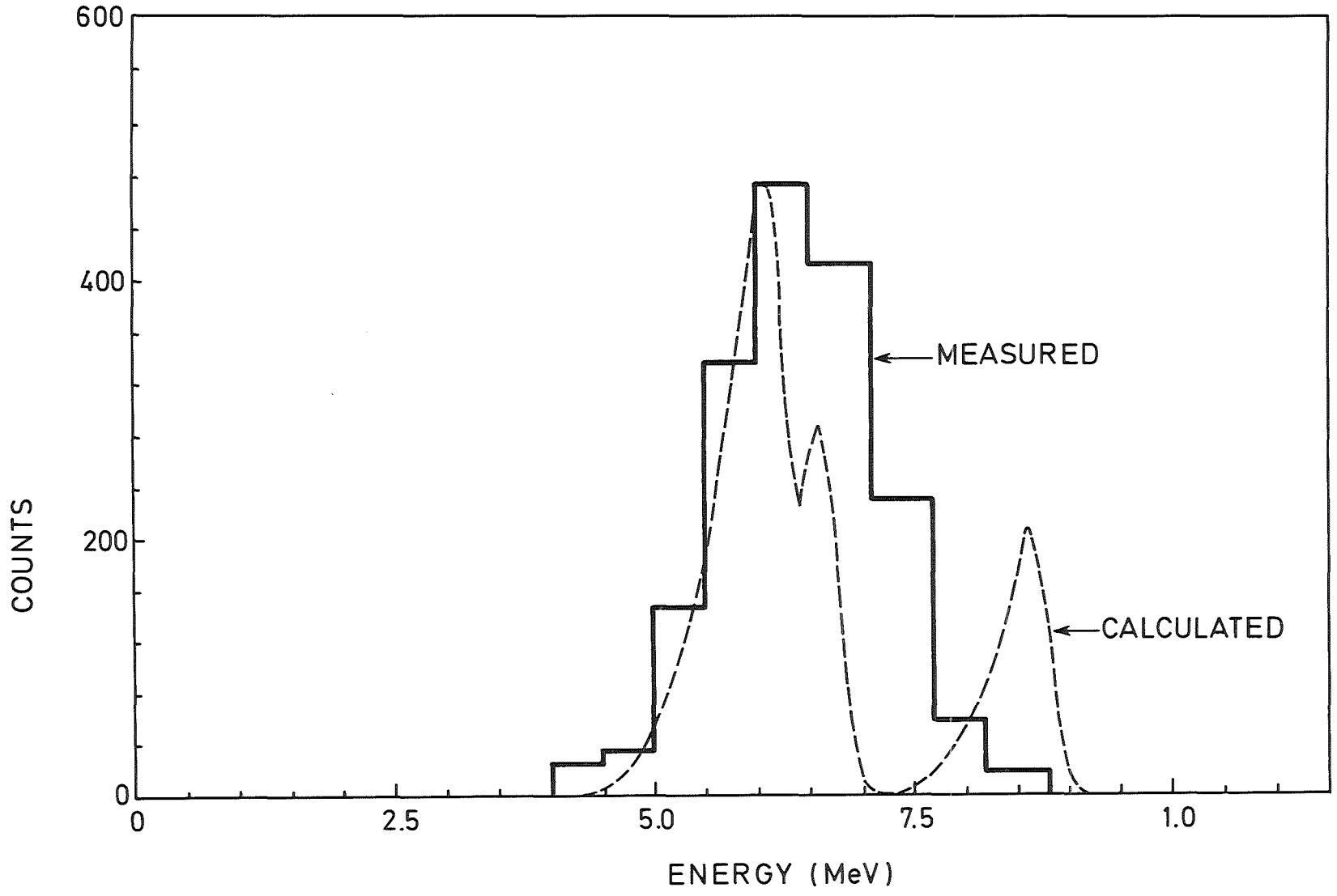

Fig. 17: Calculated and measured α-spectra in the KfK dosemeter after chemical etching of CR 39 PM for thoron and its daughter nuclides

is no maximum observed at 8.6 MeV. This loss in tracks at this energy could be either due to high level of humidity or due to the non-equilibrium of the daughter nuclides over the short irradiation time of 1 hour. A check of the spectrum using the surface barrier detector was not possible due to lack of time.

4. CONCLUSION

The conditions for optimum α-energy discrimination by ECE using CPE time or ECE track diameter are as follows:

- at 60° C in 6 M KOH
- at 15 $kVcm^{-1}$ for 2 hours.

The CR 39 PM material appears to be a better detector for α-energy discrimination than CR 39 AA as the background track density is lower and a sharper discrimination of α-energy is obtained using either CPE time or ECE track diameter.

Discrimination of α-energy using CPE time not only gives the energy of the α-particle but also the relative contribution in % of each α-energy particle. However, this discrimination becomes less distinct if the energy separation is $\leq$ 0.5 MeV. In this case, only the range of energy can be measured and no information is available regarding the relative contribution in %.

Using the KfK radon dosemeter, the estimated spectrum of the daughter nuclides from thoron gas using the four methods, i.e. ECE, chemical etching, surface-barrier detector and Monte Carlo calculation, were in close agreement. The spectrum of thoron gas and its daughter nuclides from the KfK dosemeter obtained from Monte Carlo calculation and chemical etching using Somogyi's equation do not agree at the high energy of 8.6 MeV. The discrepancy may probably due to the non-equilibrium between parent and daughter nuclides over the short irradiation time of 1 hour.

In laboratories where facilities for ECE are not available, chemical etching does provide reliable but also more information than ECE regarding the energy spectrum of α-particles. The only drawback is that it is tedious and time consuming.

5. ACKNOWLEDGEMENT

I wish to thank Mr. E. Piesch and Dr. M. Urban for their friendly assistance and discussion. Useful discussions and suggestions by Dr. Al-Najjar are deeply appreciated. My thanks are also to Mr. Reinhardt in the designing and building of the irradiation chamber. Finally, I would like to thank Mr. Lachmann for drawing the figures and Frau Krug in typing my report.

I am indebted to Universiti Sains Malaysia in granting my sabatical. Financial support through the Ida Smedley Maclean Fellowship awarded by the IFUW is gratefully acknowledged.

REFERENCES

(1) Abdel Naby A., Pálfalvi J. and Durrani s.A., Alpha-particle spectrometnry with CR-39 using combined chemical and electrochemical etching, Nucl. Tracks and Radiat. Measurement 12, 205-21), 1986.

(2) Al-Najjar S.A.R., Balcazar-Gareia M. and Durrani S.A., A Multi-Detector Electrochemical Etching and Automatic Scanning System. Nucl. Track Detection 2, 215-220, 1978.

(3) Al-Najjar S.A.R., Bull R.K. and Durrani S.A., Electrochemical Etching of CR 39 Plastic: Applications to Radiation Dosimetry, Nucl. Tracks 3, 169-183, 1979.

(4) Al-Najjar S.A.R., Detection of Neutrons and Charged Particles by Conventional and Electrochemical Etching of Polymeric Nuclear Track Recorders, PhD Thesis, University Birmingham, 1982.

(5) Amin S.A. and Henshaw D.L., Effect of Various Etching Solutions on the Response of CR 39 Plastic Track Detector, Nucl. Instr. Methods 190, 415-421, 1981.

(6) Benton E.V. and Collver M., Registration of Heavy Ions During the Flight of Gemini VI, Health Physics 13, 495-500, 1967.

(7) Blanford E.G., Walker R.H. and Wefel J.P., Calibration of Plastic Track Detectors for Using cosmic Ray Experiments, Rad. Effects 5, 41-45, 1970.

(8) Cartwright B.G., Shirk E.K. and Price P.B., Nuclear - Track Recording Polymer of Unique Sensitivity and Resolution, Nucl. Instr. Methods 15, 457-460, 1978.

(9) Cross W.G., Arneja A. and Ing H., Effect of Pre-Etching on the Registration in CR 39 of Elctrochemically-Etched Tracks of Protons and Alpha Particles of Different Energies, Nucl. Tracks and Radiat. Measurements 8, 109-112, 1984.

(10) Durrani S.A. and Al-Najjar S.A.R., The Relationship Between the Pre-Etched Track Length and the ECE Track-Spot Size, Nucl. Tracks and Radiat. Measurements 12, 211-214, 1986.

(11) Fleischer R.L. and Price P.B., Tracks of Charged Particles in High Polymers, Science 140, 1221-1222, 1963.

(12) Fleischer R.L., Price P.B. and Walker R.M., Solid State Track Detectors Applications to Nuclear Science and Geophysics. Ann. Rev. Nucl. Sc. 15, 1-28, 1965.

(13) Frank A.L. and Benton E.V., High Energy Neutron Flux Detection with Dielectric Plastic, Rad. Effects 3, 33-37, 1970.

(14) Green P.F., Ramli A.G., Al-Najjar S.A.R., Abu-Jarad F. and Durrani S.A., A Study of Bulk-Etch Rates and Track-Etch Rates in CR 39, Nucl. Instr. and Methods 203, 551-559, 1982.

(15) Griffith R.v., Fisher J.C. and Harder C.A., LLL Development of a combined Etch Track - Albedo Dosimeter. 6th ERDA Workshop on Personnel Neutron Dosimetry, Oak Ridge, PNL-2449/UC - 48, 105-117, 1977.

(16) Gruhn I.W., Li W.K., Benton E.V., Bason R.M. and Johnson C.S., Etching Mechanism and Behaviour of Polycarbonates in hydroxide solution - Lexan and CR 39. Proc. 10th IC SSNTD Lyon, Pergamon, 291-301, 1979.

(17) Hassib G.M., Tuyn J.W.M. and Dutrannois J., On the electrochemical Etching of Neutron-Induced Tracks in Plastics and its Application to Personnel Neutron Dosimetry, Proc. 9th ICSSNTD Munich, Pergamon, 905-916, 1976.

(18) Hassib J.M., A Pre-Electrochemical Etching Treatment to Improve the Detection of Neutron Recoil Track Detectors, Nucl. Track Detection 3, 45-52, 1979.

(19) Sohrabi M., The Amplification of Recoil Particle Tracks in Polymers and its Applications in Fast neutron Personnel Dosimetry, Health Physics 27, 593-600, 1974.

(20) Somogyi G. and Schlenk B., The application of Solid State Track Detector for Measuring α-Particle Angular distribution in Nuclear Reaction, Rad. Effects 5, 61-68, 1970.

(21) Somogyi G., A Study of the Basic Properties of Electrochemical Track Etching, Proc. 9th ICSSNTD Munich, Pergamon, 284-295, 1976.

(22) Somogyi G., Processing of Plastic Track Detectors, Nucl. Track Detection 1, 3-18, 1977.

(23) Somogyi G. and Hunyadi F., Etching Properties of the CR 39 Polymeric Nuclear Track Detector, Proc. 10th INCSSNTD, Lyon, Pergamon, 443-452, 1979.

(24) Somogyi G., Development of Etched Nuclear Tracks, Nucl. Instr. and Methods 173, 21-429, 1980.

(25) Sohrabi M. and Khajeian E., Effects of alpha Energy and Track Density on the Electrochemical Etching Response of Alpha and Recoil Tracks in Polycarbonate, Nucl. Tracks and Radiat. Measurements 8, 113-116, 1984.

(26) Tommasino L., Electrochemical Etching Track Detectors by Pulse and Sinusoidal Wave Forms, Le Collogue Inter. Photographic Corpusculaire Barcelone, 213-218, 1970.

(27) Urban M. and Piesch E., A Passive Radon Dosimeter For Survey Programs In Dwelling, 11th Int. Conf. on SSNTD, Bristol 1981.

(28) Urban M., Passive One-Element Track etch Dosemeter für simultaneous Measurement of Radon, Thoron and Decay Products in Air. Nuclear Tracks 12, 685-688, 1986.

(29) Williams I.R., Monte Carlo Calculations of Source-To-Detector Geometry. Nucl. Instr. and Methods 44, 160-162 1966.

APPENDIX

Programme for Monte Carlo Calculation of Energy Spectrum From Daughter Nuclides Plated out onto the walls of the KfK Radon Dosemeter.

```
10   PRINT "SOURCE CO-OD PROGRAM"
20   OUTPUT PRT; "SOURCE CO-OD PROGRAM"
30   H = 0
40   DIM E(100), S(100)
50   FOR N = 1 TO 100
60   E(N) = 0
70    S(N) = 0
80   NEXT N
90   DIM A(9)
100  FOR B = 1 TO 9
110  A(B) = 0
120  NEXT B
130  RANDOMIZE
140  READ R1,R2
150  P = PI
160  FOR IL = 1 TO 10000
170    K = INT(RND*100)
180    IF (K≦36) THEN EI = 6.1
190    IF (K>36) THEN EI = 8.8
200    PI = RND* (P/2.0)
210    TI = RND*2*P
220    X0 = RI*SIN(PL)*COS(TI)
230    Y0 = RI*SIN (PI)*SIN(TI)
240    ZO = RI*COS(PI)
250    P2 = (RND + 1.0)*P/2.0
260    T2 = RND*2.0*P
270    L = ZO/SIN(P2-P/2.0)
```

```
280      XI = XO + L*SIN(P2)*COS(T2)
290      YI = YO + L*SIN(P2)*SIN(T2)
300      ZI = ZO + L*COS(P2)
310  IF  (ZI>.001) THEN 230
320      D = SQR(XI*XI + YI*YI)
330      IF (D≦R2) THEN 180
340      GOTO 190
350      H = H + 1
360      A2 = (P2/P)*180
370          B = INT(A2/10.0)
380          A(B-9) = A(B-9) + 1.0
390      LI = .32*EI^(3/2)
400      E2 = (((LI-L/10)/.32)^2)^(1/3)
410      N = INT (E2*10)
420  E(N) = E(N) + 1.0
430  NEXT I1
440  MAT S = (0)
450      FOR I = 4 TO 96
460      S(I-3) = S(I-3) + E(I)*-0044
470      S(I-2) = S(I-2) + E(I)*.054
480      S(I-1) = S(I-1) + E(I)*.242
490          S(I) = S(I) + E(I)*.399
500      S(I + 1) = S(I + 1) + E(I)*.242
510      S(I + 2) = S(I + 2) + E(I)*.054
520      S(I + 3) = S(I*3) + E(I)*.0044
530  NEXT I
540  P9 = H*.5/10000
550  PRINT "PROBABILITY IS", P9
560  OUTPUT PRT; "PROBABILITY IS"; P9
570  PRINT "HIT IS", H, "ITERATION NO IS", I1
```

```
580  OUTPUT PRT; "HIT IS", H, "INTERATION NO IS", I1
590  FOR B = 1 TO 9
600  PRINT B,A(B)
610  OUTPUT PRT; B,A(B)
620  NEXT B
630  FOR N = 1 TO 100 STEP 5
640  PRINT N, E(N),E(N + 2), E(N + 3),E(N + 4)
650  OUTPUT PRT; N,E(N), E(N + 1),E(N + 2),E(N + 3), E(N + 4)
660  NEXT N
670  FOR I = 1 TO 100 STEP 5
680  PRINT I, S(I),S(I + 1),S(I + 2), E(I + 3), S8I + 4)
690  OUTPUT PRT; I,S(I), S(I + 1),S(I + 2), S(I + 3), S(I + 4)
700  NEXT I
710  STOP
720  PRINT "Z CO-ORD IS", ZI
730  OUTPUT PRT; "Z CO-ORD IS", ZI
740  PRINT "INTERATION NO IS", I
750  OUTPUT PRT; "INTERATION NO IS", I
760  STOP
770  END
```